Magnetic anisotropies and magnetotransport in CeH_2/Co multilayers

T. Nawrath,* B. Damaske, O. Schulte, and W. Felsch
I. Physikalisches Institut, Universität Göttingen, Bunsenstrasse 9, 37073 Göttingen, Germany
(Received 8 July 1996; revised manuscript received 12 September 1996)

Measurements of the magnetization were performed between 4.2 and 300 K on a series of periodically stacked layers of cerium hydride and cobalt prepared by reactive ion-beam sputtering. X-ray reflectometry shows that the interfaces are sharp with a rms roughness of nominally one atomic layer. In the ground state at low temperatures, for Co-layer thicknesses up to 17 Å, the magnetization is spontaneously oriented perpendicular to the layer planes in a multidomain configuration. A phenomenological analysis of the measured magnetic anisotropy energy reveals that the out-of-plane orientation of the magnetic easy axis is the result of a strong interface anisotropy which overcomes the shape anisotropy of the Co layers and of an additional volume anisotropy. Possible mechanisms behind the surface and volume anisotropies are discussed. Between 50 and 100 K, the magnetization turns into the layer planes in a continuous transition. The saturation magnetization, the spin-wave parameter describing its temperature dependence and the anisotropy energy vary continuously through the transition from the crystalline fcc phase to the amorphous phase of the Co sublayers near 20 Å. This reveals the close relationship between the electronic configurations of amorphous and fcc Co. The magnetization measurements are supplemented by measurements of the anisotropic magnetoresistance and the extraordinary Hall effect. The extraordinary Hall coefficient shows contributions from skew scattering and side jump processes and scales with the ordinary electrical resistivity. [S0163-1829(97)07405-5]

I. INTRODUCTION

The lasting interest in the magnetic anisotropies of ultrathin films and multilayers is largely motivated by the tendency of the easy axis of magnetization to be oriented perpendicular to their plane.[1] It is clear that such anisotropies have the same origin as the magnetocrystalline anisotropy in bulk magnetic materials: the spin-orbit interaction which couples the spin magnetic moment to the lattice. Greatly enhanced values of the orbital magnetic moment L_z were predicted for transition metal monolayers[2] and for magnetic multilayers,[3] and indeed, large values of L_z have been observed recently, for example, on Co/Pd and Co/Pt multilayers by measurements of x-ray magnetic circular dichroism.[4] Furthermore, a correlation has been established experimentally in a Au/Co/Au sandwich structure between the anisotropy of the Co orbital magnetic momentum and the measured anisotropy energy[5] as predicted theoretically.[2,3] First-principles calculations of the magnetic anisotropy energy have been reported for a few systems only.[6] They permit one to conclude that the anisotropy energy depends on the nature of the material adjacent to the magnetic layer. The analysis of experimental results is, as in the present paper, more or less based on phenomenological approaches which separately consider contributions to the magnetic anisotropy energy ascribed to volume (K_V) and surface or interface (K_S) terms.[7] While K_V is largely composed of magnetostatic energy (shape or demagnetization anisotropy) favoring in-plane magnetization, K_S may support a perpendicular orientation of the magnetization and may play a crucial role in determining the magnetic easy axis; it has been associated frequently with Néel's surface anisotropy, originating in the broken symmetry at the film boundaries.[8] But the microscopic origin of K_S has remained largely obscure.

For a number of ultrathin layers and layer systems, the magnetization has been found to exhibit a thermally activated transition from a perpendicular orientation at low temperatures to an in-plane orientation at higher temperatures.[9–11] This has stimulated considerable activity[12] to calculate the anisotropic part of the free energy which determines the easy magnetization direction. It has been argued[13] that the entropy connected with the magnetization direction may significantly contribute to the free energy at higher temperatures and hence provide a driving mechanism for the reorientation transition. It is an open question if this transition presents a phase transition.[14] The vanishing of the remanent magnetization in the vicinity of the reorientation transition observed for ultrathin films and wedges of Fe grown on Ag(100) (Ref. 11) has raised the question of a possible loss of magnetic long-range order near this transition, as a consequence of the mutual compensation of the magnetic anisotropies and the well-known Mermin-Wagner theorem,[15] stating that an isotropic two-dimensional Heisenberg system does not order magnetically at finite temperature. But it is more likely that the disappearance of the remanence mirrors the formation of a magnetic domain configuration in the layers.[9–11,16] This is supported by direct domain observations.[17] Theoretical work dealing with ultrathin magnetic films[18–20] and multilayers[21] has shown that in the case of a perpendicular magnetic easy axis frequently a configuration with up and down magnetized domains is the energetically preferred ground state. Such domains, irregular in shape or in the form of a stripe pattern, in some cases with extensions below the micrometer level, have been observed experimentally, for example, for a number of ultrathin ferromagnetic films by spin-polarized scanning electron microscopy,[17] or by magnetic force microscopy on Co/Pd multilayers.[22] Details depend sensitively on the magnetic parameters (exchange, anisotropy), layer thickness and temperature. The dynamics of domain formation have been stud-

 © 1997 The American Physical Society

ied recently in ultrathin Fe/Ag(100) films by measurements of the time-dependent decay of the remanent magnetization just below the reorientation transition temperature.[23]

In this paper, we investigate the magnetic anisotropy of a multilayer structure combining cobalt and cerium hydride, CeH_x/Co. We shall demonstrate that for sufficiently low Co-layer thicknesses and temperatures this system presents an easy axis of magnetization along the growth direction. The hydrogen content x is close to 2, CeH_2 is paramagnetic in the temperature range investigated and a poor metallic conductor; it is close to a transition to a semiconducting state.[24] The study extends previous work performed on the multilayer system CeH_2/Fe which exhibits very special properties if Fe is grown in the unusual bcc-(111) texture on the (111) textured fcc-CeH_2 sublayers. A strong surface anisotropy, together with a magnetostatic interaction within a magnetic multidomain structure, leads to a perpendicular orientation of the magnetic easy axis;[25] at a critical temperature, the easy axis turns into the layer planes.[26] This behavior is outstanding as compared to other rare-earth-iron multilayers, like Tb/Fe (Refs. 27 and 28) or Nd/Fe,[29,30] because the out-of-plane magnetic configuration is truly perpendicular, it persists up to remarkably large Fe-layer thicknesses, and the reorientation transition occurs in a narrow temperature range. Furthermore, a recent study by polarized neutron reflectometry has shown that in the state with an in-plane magnetization orientation, CeH_2 provides a magnetic coupling between adjacent Fe layers, generating a long-range magnetic superstructure.[31] The presence of hydrogen in the rare-earth layers is essential for these phenomena, since in bare Ce/Fe layers the magnetization is always confined to the layer planes and a Fe interlayer coupling does not occur. This may be related to the different electronic configuration of cerium at the interfaces in these structures, which presents a mixed-valent character (like in bulk α-phase Ce) in the Ce/Fe system,[32] but a more normal trivalent character (like in γ-phase Ce) in the CeH_2/Fe system.[33] It appears that the perpendicular magnetic anisotropy in the latter system is bound to the (111) texture of the bcc-Fe sublayers; for the (110) texture, the preferred orientation of the magnetization lies in the layer planes,[34] and in the hydrogen-free Ce/Fe system (111) oriented growth cannot be accomplished. Note that LaH_2/Fe multilayers with (111)-textured bcc Fe show an in-plane magnetic easy axis.[31] This raises the question about the role of the Ce-4f local moment, in particular of its orbital part, in the phenomenon of perpendicular magnetic anisotropy in the CeH_2-based layered system.

The study of the CeH_2/Co multilayers presented here comprises a structural characterization, measurements of the bulk magnetization, of the anisotropic magnetoresistance and the extraordinary Hall effect. At low thicknesses, the Co sublayers grow in an amorphous structure. This permits to study the magnetic properties of pure amorphous Co. It will be shown that these properties vary smoothly through the crystalline-to-amorphous transition. The magnetotransport properties, providing supplementary information on the magnetic anisotropy of the layers which is more directly reflected in the magnetization curves, are interesting on their own. In particular, it is not clear if the usual scaling relation between the extraordinary Hall resistivity and the ordinary resistivity generally holds in heterogeneous layered magnetic systems.[35]

II. SAMPLE PREPARATION

The multilayers CeH_x/Co were prepared by computer-controlled reactive ion-beam sputtering of Ce ($3N$) and Co ($5N$) targets at room temperature using argon in an ultrahigh vacuum chamber, at a hydrogen partial pressure of 8×10^{-6} mbar. Both gases were of high purity ($6N$). The base pressure was below 5×10^{-10} mbar prior to the introduction of hydrogen. Partial pressures of reactive gases (e.g., O_2, N_2, H_2O, or CO) were below 10^{-10} mbar during the deposition process. This means, in particular, that the formation of hydrocarbons by the reaction of CO and hydrogen with Co as a catalyst[36] if any, must be at a negligible level. The hydrogen content of the multilayers was determined by the nuclear resonance reaction $^1H(^{15}N, \alpha\gamma)^{12}C$.[25] While bulk Ce forms very stable hydrides, the solubility of hydrogen in bulk Co is very low [the enthalpy of mixing with hydrogen is negative and large for Ce (≈ -70 kJ/mol H for dilute solutions, and ≈ -100 kJ/mol H for the formation of CeH_2) but positive for Co ($\approx +20$ kJ/mol H for the dilute case) (Ref. 37)]. Therefore, it is reasonable to assume that *only the Ce sublayers* absorb hydrogen, i.e., that the multilayers grow in the form $[CeH_x/Co]\times n$. The ^{15}N method then yields a hydrogen content x of CeH_x close to 2. It is clear that knowledge of the hydrogen concentration profile in the multilayers is a crucial point; it will be addressed more closely in Sec. III below. Si(100) and $Al_2O_3(1120)$ were used as substrates (the latter ones for the measurements of the transport properties). They were precoated with a 40 Å thick buffer layer of Cr to warrant independence of the multilayer properties from the substrate material. Growth rates varied from 0.3 Å/s for CeH_2 to 0.6 Å/s for Co. Two series of multilayers were prepared, with a total thickness near 2000 Å: one with constant CeH_2 layer thickness of 15 Å and Co layer thicknesses between 11 and 53 Å, the other with a constant Co layer thickness of 24 Å and CeH_2 layer thicknesses between 9 and 34 Å. To prevent oxidation on exposure to atmosphere, the samples were covered with a layer of 100 Å Cr.

III. STRUCTURAL PROPERTIES

The structure of the multilayers was characterized by x-ray diffractometry with Cu-K_α radiation at small and large scattering angles, mainly in Θ-2Θ geometry, and by reflection high-energy electron diffraction (RHEED) diagrams taken *in situ*. Below a critical thickness of about 20 Å for Co and about 15 Å for CeH_2, the individual layers grow in an amorphous structure. This is reflected in diffuse intensities in the high-angle x-ray spectra and the RHEED diagrams. Amorphous growth in layered heterostructures combining rare-earth and transition metals is a well known and frequently observed phenomenon which has been related to the constraints imposed by the mismatch between the sublayer lattices at the interfaces.[38,39] For the CeH_2/Co system, where the crystalline phases of both sublayers are fcc, the misfit

between the (bulk) lattice constants amounts to $[a(CeH_2)-a(Co)]/a(Co)=57\%$.

Above the critical thickness the individual layers present a polycrystalline structure with a preferred orientation along the growth direction. The diffraction diagrams show a fcc(111) texture for CeH_2, and a fcc(111) or hcp(002) texture for Co. The Θ-2Θ geometry does not reveal the stacking sequence, but as we shall argue below, the analysis of the magnetic anisotropy allows to exclude hcp Co. Rocking curves around the (111) reflections of both CeH_2 and Co yield full widths at half maximum (FWHM) of typically 10°. The structural coherence length along the direction of the multilayer normal, as determined from the linewidths of the (111) Bragg peaks, is limited by the thickness of the individual layers which means that growth is not coherent across the interfaces. This is corroborated by the absence of superlattice satellite reflections near the Bragg reflections.

The ^{15}N nuclear reaction analysis of the hydrogen concentration in the multilayers is limited by a depth resolution of the order of 100 Å. Thus in our multilayer samples, as in other cases, the individual layers cannot be resolved, only the average concentration is measured. To interpret the result we assume, as we have indicated in Sec. II, that due to the very different hydrogen solution or reaction enthalpy hydrogen is confined to the Ce layers while the Co layers are essentially free of hydrogen. Admittedly, this may only be true in a crude approximation, since it is well known that the behavior of hydrogen in a thin layer may deviate strongly from the behavior in a bulk solid.[40] Let us note that hydrogen charging of layered systems is rather unexplored up to now[41] and presents a challenge for experimentalists. Unfortunately, x-ray diffraction is not accurate enough in our case to examine directly if there is any uptake of hydrogen by the Co sublayers in the multilayers, since the Bragg reflections are broad due to the small thickness or amorphous structure. Single 2000-Å-thick Co layers prepared under the same conditions but with and without hydrogen in the recipient, which show sharper Bragg peaks, present the same lattice constant within an accuracy of $\sim 5\times 10^{-4}$. With the hydrogen-induced volume expansion taken from the literature[42] this puts an upper limit of $\sim 1\%$ for the concentration of hydrogen in these layers. Further information which is more indirect can be obtained by a comparison with the hydrogen uptake of the Fe sublayers in Nb/Fe multilayers with thick individual layers,[43] since the hydrogen solution enthalpies of Fe and Co, and the Fe-H and Co-H phase diagrams[44] are very similar. It results that the uptake of hydrogen in the Fe layers is negligible. Employing the argument of the very different solution enthalpies for hydrogen in the two metals, the authors state that this result should hold for thin Fe layers, too. By the same reasoning we may hypothesize that in our multilayer samples there is essentially no hydrogen in Co sublayers. The same conclusion was drawn for the CeH_x/Fe multilayers investigated previously.[25] But it is clear that a direct proof would be highly desirable, as well as accurate experimental information on the concentration profile of hydrogen immediately at the interfaces between the two metals.

Particular attention has been devoted to the structure of the interfaces. Figure 1 shows the small-angle x-ray reflectometry diagrams of four multilayers. All samples show a number of superlattice reflections which points to the presence of sharp interfaces and a well-ordered layering of the constituent metals. To quantify interfacial roughness, the data were analyzed by employing results of the dynamical scattering theory.[45] Good fits are obtained for rms roughnesses (FWHM) between 2.2 and 2.8 Å. In particular, the structure of the Co layers (amorphous for the thicknesses 11 and 14 Å, crystalline for 20 and 24 Å) does not have a noticeable influence on the interfacial roughness.

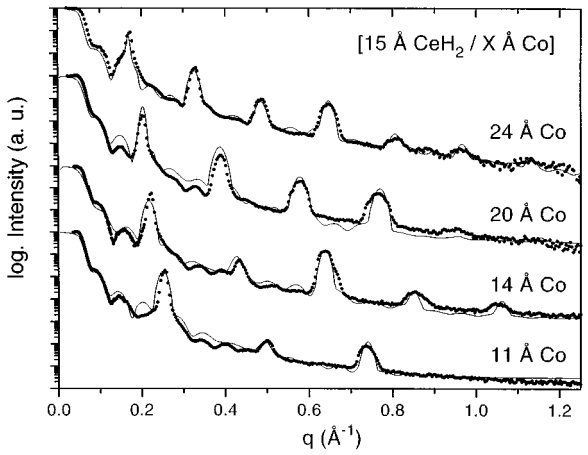

FIG. 1. Low-angle x-ray reflectometry diagrams of CeH_2/Co multilayers (total thickness 2000 Å). Solid curves: fits based on dynamical scattering theory. The curves have been displaced vertically.

IV. MAGNETIZATION AND MAGNETIC ANISOTROPY

The magnetization of the samples was measured by a vibrating-sample magnetometer between 4.2 K and room temperature, in magnetic fields up to 50 kOe applied parallel and perpendicular to the layer planes. All CeH_2/Co samples with Co-layer thicknesses t_{Co} above 11 Å show ferromagnetic behavior in the temperature range covered. Let us mention that according to magnetization measurements in low fields there is no evidence for magnetic interlayer coupling contrary to the CeH_2/Fe multilayers.[31] Figure 2 shows, as a representative example, the magnetization curves of the multilayer [15 Å CeH_2/14 Å Co]×77 at 4.2 K and 100 K for two orientations of the applied magnetic field. Obviously,

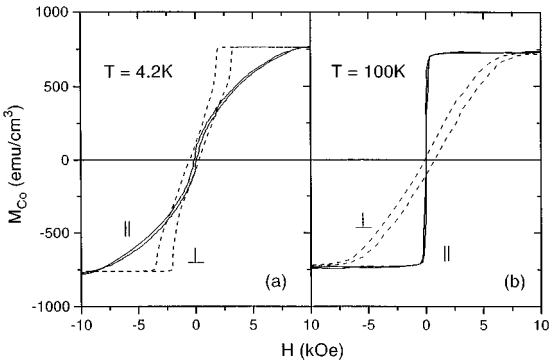

FIG. 2. Magnetization curves of a multilayer [15 Å CeH_2/14 Å Co]×77 in a magnetic field H applied parallel (full line) and perpendicular (dashed curve) to the layer plane at 4.2 (a) and 100 K (b). The magnetization is referred to the Co volume.

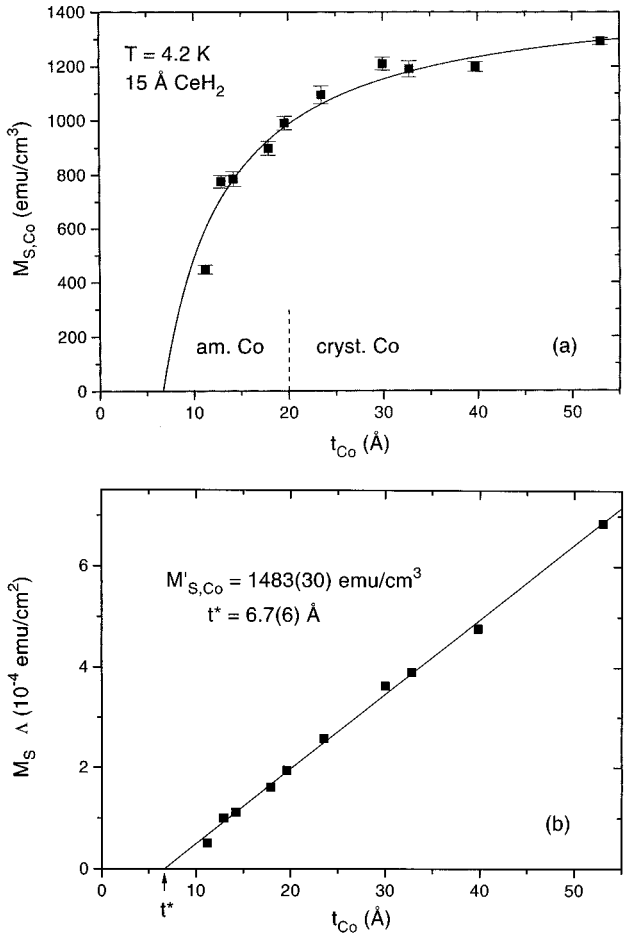

FIG. 3. (a) Saturation magnetization $M_{S,\mathrm{Co}}$ (referred to the Co part) of CeH_2/Co multilayers with 15-Å-thick CeH_2 layers at 4.2 K as a function of the Co-layer thickness t_{Co}. At $t_{\mathrm{Co}}=20$ Å, the Co layers undergo an amorphous-to-crystalline transition. Solid line: fit to Eq. (1). (b) Saturation magnetization M_S (referred to the total volume) of CeH_2/Co multilayers (CeH_2-layer thickness 15 Å) times periodicity length $\Lambda=t_{\mathrm{CeH}}+t_{\mathrm{Co}}$ at 4.2 K vs Co-layer thickness t_{Co}. The straight line represents Eq. (1).

these curves reveal a crossover from a state with an out-of-plane magnetic anisotropy prevailing at low temperatures to a state with in-plane anisotropy at higher temperatures. This will be discussed in detail below. We first focus on the magnetization.

The measured saturation magnetization of all samples, referred to the total Co part, $M_{S,\mathrm{Co}}$, is noticeably reduced relative to the literature value of bulk fcc Co (1460 emu/cm^3 at 4.2 K), it decreases with decreasing t_{Co}; this can be seen in Fig. 3(a). The reduction is the result of an interface effect: to show this, we have plotted in Fig. 3(b) the product of the saturation magnetization referred to the total volume of the samples, M_S, and the multilayer periodicity length Λ as a function of t_{Co}; Λ and t_{Co} are derived from the x-ray spectra and their simulation. The data obey the relation

$$M_S\Lambda = M'_{S,\mathrm{Co}}(t_{\mathrm{Co}}-t^*) \tag{1}$$

with $M'_{S,\mathrm{Co}}=(1483\pm30)$ emu/cm^3 and $t^*=(6.7\pm0.6)$ Å [Fig. 3(b)]. The result means that the reduction of the magnetization is due to a magnetically ''dead'' zone in the

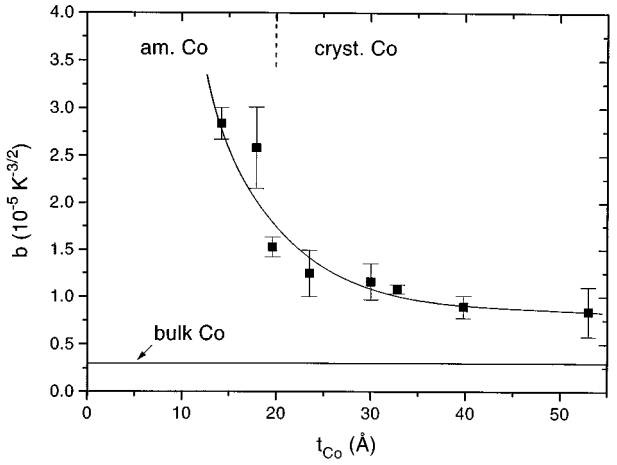

FIG. 4. Spin-wave parameter b defined in Eq. (2) of CeH_2/Co multilayers (CeH_2-layer thickness 15 Å) as a function of the Co-layer thickness t_{Co}. The error bars result from least-squares fits to Eq. (2). Line: guide to the eye. Horizontal line: value of bulk fcc Co: $b=3.0\times10^{-6}$ K$^{-3/2}$.

Co layers at each interface, with an extension $t^*/2$ corresponding to nominally somewhat more than one monolayer. This value is only slightly larger than the rms interfacial roughness resulting from x-ray scattering (Sec. III), which suggests that the dead zone may be due to a hybridization of the Co-3d and the CeH_2-5d electronic states in the intermixed region. In the remaining part of the Co sublayers with thickness $t'_{\mathrm{Co}}=(t_{\mathrm{Co}}-t^*)$ and saturation magnetization $M'_{S,\mathrm{Co}}$ we have the same ordered magnetic moment as in bulk Co, even for low values of t_{Co}. Between 4.2 and 300 K, the temperature dependence of $M'_{S,\mathrm{Co}}$ obeys a Bloch spin-wave law for a three-dimensional ferromagnetic sample,

$$M'_{S,\mathrm{Co}}(T)=M'_{S,\mathrm{Co}}(0)(1-bT^{3/2}). \tag{2}$$

The spin-wave parameter b, which is related to the exchange interaction experienced by the Co spins, is shown in Fig. 4 as a function of the Co-layer thickness t_{Co}. All values of b are distinctly enhanced compared to the literature value of fcc Co [$b=3.0\times10^{-6}$K$^{-3/2}$ (Ref. 46)].

The saturation magnetization M_S and the spin-wave parameter b of the CeH_2/Co multilayers vary continuously through the transition from the crystalline to the amorphous state of the Co layers at $t_{\mathrm{Co}}\approx20$ Å (Figs. 3 and 4). This is in contrast to the behavior of the CeH_2/Fe system,[34] or of other multilayers with iron, like, for example, Y/Fe,[47] Ce/Fe,[48] or La/Fe,[49] where the crystalline-to-amorphous transition in the Fe sublayers is accompanied by an abrupt reduction of the saturation magnetization and Curie temperature, and by the appearance of a noncollinear spin structure in Fe. The coercive fields H_c in the CeH_2/Co multilayers amount to a few 10 Oe at 4.2 K for all values of t_{Co}. On the other hand, in the CeH_2/Fe system H_c adopts a maximum of about 1 kOe at the amorphous-crystalline boundary of the Fe sublayers.

For more than two decades, the magnetism of amorphous Fe and Co is an important issue of experimental[50] and theoretical research.[51–53] It appears by now that the very different magnetic properties of these amorphous metals are an image of the different electronic structures of the bulk crystalline

phases and the different sensitivity of their magnetic parameters to variations of the local environment parameters. The electronic configurations of amorphous Fe and amorphous Co, which both present a nearly close-packed structure, are very similar to those of the fcc phases of these metals. Hence, their magnetic behavior is strongly correlated with the dependence of the magnetic moments and exchange-coupling constants on the interatomic distances in the fcc phases.[52] In fact, the peculiarities in the magnetic properties of amorphous Fe result from strong magnetovolume effects which are well known to play a decisive role in the magnetic behavior of the fcc phase of this metal in which both ferro- and antiferromagnetic coupling may occur. In fcc and hence amorphous Co, which is of interest here, magnetovolume effects are comparatively weak, which leads to significant differences in the magnetic properties with respect to Fe. Recent theoretical work[52] has shown that the most important factor influencing the magnetic properties of amorphous Co is the symmetry of the arrangement of the near neighbors. The authors educe a narrow distribution of the magnetic moments with an almost collinear order and, as a result of the magnetic energy gain due to the structural disorder, an enhanced ferromagnetic exchange interaction as compared to fcc Co. The average ordered magnetic moment in the ground state of amorphous Co calculated by them and others[54,55] coincides with that calculated for fcc Co within 3%. This is in good agreement with experimental results obtained from extrapolation in Co-rich amorphous alloys,[50,56] and also with the results in the present work where pure amorphous Co is stabilized in a multilayer structure.

The enhancement of the exchange-coupling constant J resulting from theory[52,55] translates into an increase of the Curie temperature T_c of amorphous Co with respect to the fcc phase if the mean-field expression $T_c \propto J$ is used. In fact, an extrapolation of the recently obtained T_c data of amorphous Co-Y alloys[56] to pure amorphous Co yields a value which is about 30% higher than that of crystalline hcp or fcc Co, and a considerably reduced spin-wave parameter b. In our multilayer system CeH_2/Co, the values of b are *enhanced* as compared to bulk fcc Co for all Co-layer thicknesses, without a discontinuous change at the crystalline-to-amorphous transition (Fig. 4). This indicates, through the usual relation $b \propto J^{-3/2}$, that the exchange constant J may be *reduced*. Since the samples were not stable up to sufficiently high temperatures, it was not possible to examine how this is reflected in the Curie temperature. One may hypothesize that the exchange enhancement in amorphous Co expected from theory for bulk material is overcompensated, in the present layered system, by similar mechanisms which are conceivable to be effective in the thickness range where Co is crystalline and which may lead to magnetic softening: a change in the environmental parameters near the interfaces, possibly induced by hydrogen, or electron transfer due to hybridization of the Co-3d and CeH_x-5d states. Such hybridization effects have been shown to be important for magnetism in CeH_x/Fe multilayers.[33]

Samples with Co-layer thicknesses $t_{Co} \leqslant 11$ Å may not be saturated magnetically in the available field (50 kOe), their Curie temperatures are below 250 K. They will be disregarded in the following, i.e., the discussion will be focused on samples with $t_{Co} > 11$ Å.

The magnetization curves of the sample [15 Å CeH_2/14 Å Co]$\times$77 in Fig. 2, measured at 4.2 and 100 K in magnetic fields along the in-plane and perpendicular directions, reveal a crossover from a state with out-of-plane magnetic anisotropy to a state with in-plane anisotropy, occurring in between the two temperatures. This is evident from the relative magnitude of the magnetic saturation fields $H_S^{\perp}$ and $H_S^{\parallel}$ and its reversal as the temperature is increased: these fields are a measure of the anisotropy fields related to an in-plane and out-of-plane magnetic easy axis, respectively. The magnetization curve in the perpendicular field at 4.2 K is very similar to those measured for CeH_2/Fe multilayers which, according to ^{57}Fe Mössbauer spectroscopy, present an easy axis for the magnetization parallel to the layer normal.[25,26] We therefore assume that in the CeH_2/Co sample addressed in Fig. 2 the out-of-plane magnetic easy axis at 4.2 K is oriented along the layer normal, too. Measurements of the low-field ac magnetic susceptibility reveal that the reorientation transition of the magnetic easy axis into the layer plane occurs much more gradually with increasing temperature than in the CeH_2/Fe system. In CeH_2/Co, reorientation starts near 50 K and extends to about 100 K. The low remanence and the small hysteresis in the perpendicular magnetization curve at 4.2 K, together with its shearing from a steplike increase ideally expected along the easy direction, indicate that the perpendicular ground state of the layer is characterized by a magnetic structure consisting of domains magnetized alternately up and down along the layer normal. The kneelike feature appearing in the magnetization curve upon demagnetization from saturation, followed by a linear decrease, mirrors magnetization reversal from the field-induced perpendicular monodomain state by nucleation of reversed domains and subsequent domain-wall motion. On the other hand, the rounded shape of the in-plane magnetization curve at 4.2 K indicates that the transition from the perpendicular multidomain state to the in-plane monodomain state induced by the magnetic field is governed by rotation of the magnetization within the domains.

The values of the magnetic saturation fields $H_S^{\perp}$ and $H_S^{\parallel}$ at 4.2 K are compared in Fig. 5 for various thicknesses t_{Co} of the individual Co layers in the system [15 Å CeH_2/t_{Co}Co]$\times N$. Let us note that these fields, at least for the multilayer series with 24-Å-thick Co layers, are independent of the CeH_2-layer thickness. The curves $H_S^{\perp}(t_{Co})$ and $H_S^{\parallel}(t_{Co})$ cross at $t_{Co} \approx 17$ Å, which is the upper limit, at 4.2 K, for a perpendicular magnetic easy axis in the multilayers. This value is close to the critical thickness for the crystalline-to-amorphous transition in the Co layers. It falls into the interval of values reported for other Co-based multilayers which extends from below 10 Å to almost 20 Å.[7] The t_{Co} boundary for perpendicular anisotropy is considerably lower than the corresponding thickness found for the CeH_2/Fe multilayers with bcc-(111) texture of Fe, for which the stability of the state with a perpendicular spontaneous magnetization depends both on the Fe and CeH_2-layer thicknesses and persists, at 16 Å CeH_2, for example, even up to 50-Å-thick Fe layers.[25] In the CeH_2/Fe system, the magnetic field for perpendicular saturation, $H_S^{\perp}$, in this state closely follows, at 4.2 K, the relation

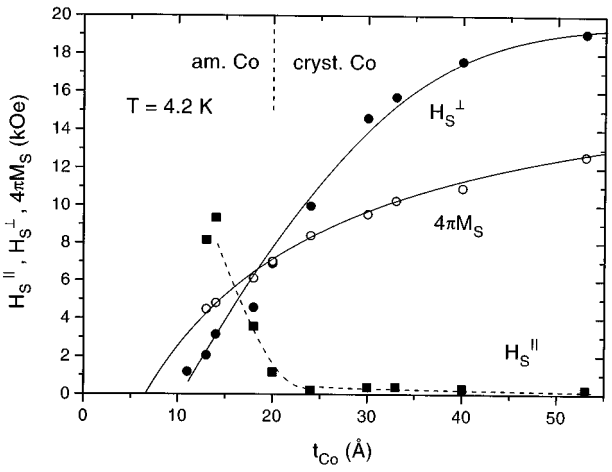

FIG. 5. Magnetic saturation fields $H_S^{\perp}$ and $H_S^{\parallel}$ deduced from the perpendicular and parallel magnetization curves, and $4\pi M_S$ of CeH_2/Co multilayers (CeH_2-layer thickness 15 Å, saturation magnetization M_S referred to the total volume) at 4.2 K as a function of the Co-layer thickness t_{Co}. Solid line through the $4\pi M_S$ data: Eq. (1). Lines through the saturation fields: guides to the eye.

$$H_S^{\perp} = 4\pi M_S \tag{3}$$

as a function of the sublayer thicknesses t_{Fe} and t_{CeH}, where M_S is the saturation magnetization referred to the *total multilayer volume*. As can be seen in Fig. 5, this is not the case for the CeH_2/Co multilayers: here, we have $H_S^{\perp} < 4\pi M_S$ at low values of t_{Co} in the perpendicularly magnetized state. The functional dependence in Eq. (3) has been derived by Suna[57] in a simple model for the perpendicular magnetic ground state of a multilayer structure. The model is based on the assumption, that a perpendicular multidomain rather than a monodomain configuration is energetically favored, which is supposed to consist of alternately polarized stripe domains. The stability of this state is brought about by the magnetostatic interaction between the domains. Within the limit that the domains are large compared to the thickness of the magnetic layers but small compared to the total thickness of the layered stack, it simply results that the multilayer behaves like a uniform medium and the magnetostatic interaction between the domains (within the magnetic and across the nonmagnetic layers) can be derived in a continuum approach. The magnetic energy per multilayer unit volume required to saturate the sample perpendicularly to the layer plane then amounts to $2\pi M_S^2$, which is the difference in energy density between the perpendicular multidomain and monodomain states. Hence, in a magnetic field applied along the layer normal, saturation is reached at $H_S^{\perp} = 4\pi M_S$. It has to be noted that, in this model, the stability of the perpendicularly magnetized ground state is entirely the result of the magnetostatic intra- and inter-layer interaction between the domains, with energy density $2\pi M_S^2$. While this appears to be predominantly the case for the CeH_2/Fe system at 4.2 K [above 16 Å of (111)-textured Fe and/or CeH_2] where the data fulfill Eq. (3),[25] the considerable reduction of $H_S^{\perp}(t_{Co})$ relative to the values of $4\pi M_S(t_{Co})$ in the perpendicular state (Fig. 5) indicates that magnetostatic interdomain interaction across the CeH_2 layers is less effective in the CeH_2/Co system in stabilizing the perpendicular magnetic state. In fact, since $H_S^{\perp}$ and $H_S^{\parallel}$ are independent of the CeH_2-layer thickness, such interaction must be of minor importance. Possibly, the lateral domain size is to large and the prerequisites for its upper limit, as required in the model of Suna[57] and apparently fulfilled in the CeH_2/Fe system, are not met. Obviously, the perpendicular magnetization state must result from other mechanisms. (At Co-layer thicknesses for which the magnetic easy axis lies in the film plane, $H_S^{\perp}$ exceeds $4\pi M_S$ as expected.)

The area enclosed by the magnetization curves for a field applied perpendicular or parallel to the layer planes (see, e.g., Fig. 2) represents the effective magnetic anisotropy energy density K_{eff}, which is a measure of the difference in energy density between the monodomain configurations with parallel and perpendicular magnetization. Because in many systems K_{eff} varies approximately with the inverse magnetic layer thickness, it has become a common (though somewhat arbitrary) practice[7] to decompose K_{eff} into a volume and a surface or interface contribution, K_V and K_S, which for the present system reads as

$$K_{eff} t'_{Co} = K_V t'_{Co} + 2K_S, \tag{4}$$

with $K_V = K_V^* - 2\pi M'^2_{SCo}$. In this phenomenological relation, we use the Co-layer thickness $t'_{Co} = (t_{Co} - 6.7\ \text{Å})$ and the magnetization $M'_{S,Co}$, both corrected for the magnetically dead zone according to Eq. (1). $(-2\pi M'^2_{SCo})$ denotes the shape anisotropy, K_V^* an additional volume contribution, and the factor 2 in front of K_S arises from the two interfaces of each layer. $K_{eff} > 0$ is assigned to the case of a perpendicular magnetic ground state, which is favored by $K_V, K_S > 0$. It must be emphasized however that if the system lowers its energy by the formation of perpendicular magnetic domains, even negative values of K_{eff} (which compares monodomain configurations only) may be compatible with a spontaneous perpendicular orientation of the magnetization. In fact, as we have mentioned above, the previously investigated multilayers CeH_2/Fe (Ref. 25) present an instructive example for a system where the perpendicular magnetic state is considerably stabilized by the interaction of the perpendicular domains in the Fe layers across the CeH_2 spacer layers. We have also argued that such a stabilization effect is quite small in the CeH_2/Co system.

Figure 6(a) shows $K_{eff} t'_{Co}$ as a function of t'_{Co} for constant t_{CeH} at different temperatures. A linear relationship according to Eq. (4) is reasonably well obeyed, except for the lowest t'_{Co} value at 4.2 K. This may indicate that a decomposition of the anisotropy energy density into a volume and interface contribution looses its meaning for very low Co-layer thicknesses in the present system. At 4.2 K, K_{eff} changes its sign at $t'_{Co} \approx 10$ Å, i.e., at $t_{Co} \approx 17$ Å, which corroborates the critical-thickness value (at this temperature) for the transition from a perpendicular to an in-plane magnetic easy axis resulting from a comparison of the perpendicular and parallel magnetic saturation fields in Fig. 5. Note that there is no discontinuous change of the data at the crystalline-to-amorphous transition near $t'_{Co} = 13$ Å, K_{eff} is not sensitive to amorphization. The values of K_S and K_V^* resulting from the fits at the various temperatures and the

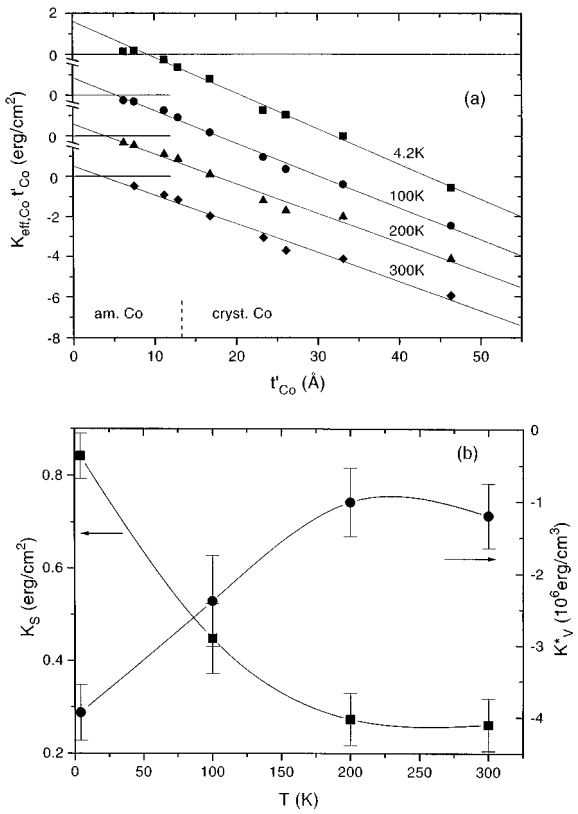

FIG. 6. (a) Product of the effective magnetic anisotropy (referred to Co), $K_{\mathrm{eff,Co}}$, and effective Co-layer thickness t'_{Co} vs t'_{Co} for CeH_2/Co multilayers (CeH_2-layer thickness 15 Å) at four selected temperatures [Eq. (4)]; the curves have been displaced vertically. (b) Temperature dependence of the interface and volume anisotropy contributions, K_S and K_V^* resulting from the straight lines fitted to the data in (a) (see text). The solid lines in (b) are guides to the eye.

subsequent subtraction from K_V of the measured temperature-dependent shape anisotropy $(-2\pi M'^2_{S,\mathrm{Co}})$, are displayed in Fig. 6(b). They both vary considerably with temperature and have different signs, hence they counteract in their mutual influence on the magnetic anisotropy of the multilayers. The positive sign and the relatively large value of the interface anisotropy K_S reveals that it is the mechanism behind this quantity which here is at the origin of the perpendicular anisotropy. At 4.2 K, we have $2K_S/t'_{\mathrm{Co}} = 17\times10^6$ erg/cm^3 for $t'_{\mathrm{Co}} = 10$ Å which is $\sim 4|K_V^*|$. The decrease of K_S with increasing temperature reflects the growing tendency for in-plane orientation of the magnetization. This orientation is supported by the negative volume anisotropy K_V^* and the shape anisotropy, K_V^* amounting up to $\sim$30% of $(-2\pi M'^2_{S,\mathrm{C0}}) = -1.38\times10^7$erg/cm^3 at 4.2 K.

The magnetic anisotropy densities in Fig. 6(b) may be compared with results found in other Co-based multilayers showing out-of-plane orientation of the magnetization.[7,58] Such a comparison can reveal trends only since it is well known that the absolute values reported in general depend on the structural properties of the interfaces.[58] The values of the interface component K_S are generally positive and range between 0.5 and 1.0 erg/cm^2, which is of similar magnitude as in the present system. But it is clear that the physical origin of K_S may be of different nature in each case; possible contributions, for example, may derive from hybridization effects in the electronic structure near the interfaces, which possibly are reflected here in the magnetically dead zone in the Co layers, or from magnetoelastic effects in the case of incoherent growth across the interfaces[59] which is realized in the present system (Sec. III).

Contributions to the volume anisotropy K_V^* which appear in addition to the shape anisotropy may be expected to result from magnetocrystalline and/or magnetoelastic anisotropies. As we have pointed out in Sec. III, the x-ray-diffraction diagrams do not permit one to identify the observed texture of the Co sublayers in the multilayer samples with CeH_2 as fcc(111) or hcp(002). The magnetocrystalline anisotropy is negligible for fcc Co and amounts to 0.56×10^7 erg/cm^3 for a hcp-Co film with the c axis along its normal. Since the observed values of K_V^* [Fig. 6(b)] are very small at room temperature as compared to the shape anisotropy and become increasingly negative towards low temperatures, it can be concluded that (i) the structure of the Co films is predominantly fcc and (ii) the observed anisotropy K_V^* is not of magnetocrystalline origin. Let us note that a comparison with K_V^* data compiled for various Co-based multilayers[7,58] is not very illuminating: a broad range of mostly positive values is reported which depend on the crystalline orientation.

A remaining possibility is to attribute K_V^* to strain in the magnetic sublayers which contributes to the total magnetic anisotropy energy density of a multilayer via magnetoelastic coupling. Quite generally, strain can be induced by various sources. Among them is lattice mismatch between dissimilar adjacent layers, or intrinsic strain arising during the growth process. K_V^* is very small at room temperature and essentially appears only at temperatures below 200 K. This suggests to identify its source with thermal strain associated with differences in the thermal expansion coefficients of the layer materials and the substrate, or with a structural distortion in the CeH_2 sublayers which has recently been observed in the CeH_2/Fe multilayers somewhat below 200 K, where it leads to a lateral expansion of the bcc-Fe lattice.[60] Let us mention that a tetragonal distortion around 200 K is a well documented property for bulk CeH_x crystals with a similar hydrogen concentration as in our layered system.[61] We tentatively hypothesize that such a mechanism is effective in the CeH_2/Co multilayers in generating a magnetoelastic contribution to the magnetic volume anisotropy of the Co sublayers. Since the effective anisotropy energy density K_{eff} and hence also K_V^* vary continuously through the crystalline-to-amorphous transition in the Co layers [Fig. 6(a)], we assume, in a first approximation, that the magnetoelastically-derived volume anisotropy energy density of the Co layers can be estimated from the expression for an isotropic medium[62]

$$K_{\mathrm{me}} = -\tfrac{3}{2}\lambda\sigma\cos^2\varphi, \tag{5}$$

where λ is the isotropic magnetostriction constant, σ is the stress related to the strain ε via the elastic modulus E by $\sigma = \varepsilon E$, and φ is the angle between the stress axis and the magnetization. Equation (5) shows that K_{me} is negative for tensile strain $\sigma > 0$ and positive magnetostriction λ and hence favors an in-plane magnetic easy axis. The problem is that λ of fcc Co is not known, in particular not for the

present multilayer structure. Extrapolation of the recently measured data[63] of Pd/Co multilayers with fcc-(111) interfacial orientation to thick Co layers, or of Pd-Co alloys to pure fcc Co yields a very *small but positive* $\lambda \geq 0$ if the relation $\lambda = (2\lambda_{100} + 3\lambda_{111})/5$ is used for the averaging procedure.[62] But this is not very conclusive since it has been recently observed[64] that λ cannot be simply transferred from bulk crystals or from other layered structures. We must conclude then that without measured data of σ and λ for the present Co-based multilayer system it cannot be decided if the measured volume anisotropy K_V^* is at least partly due to a magnetoelastic mechanism; at present, the source of K_V^* must remain unexplained even qualitatively. Let us mention that in the comparative multilayer system CeH_2/Fe a corresponding volume term does not appear, the measured magnetic volume anisotropy density K_V is entirely of dipolar origin, i.e., is a pure shape anisotropy.[25]

V. MAGNETOTRANSPORT

A. Anisotropic magnetoresistance

The magnetoresistance of the multilayers, $\Delta\rho(H)/\rho(0) = [R(H) - R(0)]/R(0)$ was measured in standard four-contact geometry, using an ac driving current of 100 μA at 117 Hz in the layer plane, and a magnetic field H directed parallel to the current (longitudinal magnetoresistance) or along the layer normal (perpendicular magnetoresistance).

Quite generally, the common anisotropic magnetoresistance (AMR) of magnetic materials (not to be confounded with the giant magnetoresistance in layered magnetic structures which has not been observed in the present system) originates from spin-orbit coupling and usually is small $[\Delta\rho(H)/\rho(0) \sim 1\%]$. Theoretical models involve anisotropic *s-d* scattering mechanisms.[65] In the following we shall demonstrate how the AMR can be used to investigate the magnetic anisotropy of thin layers. The AMR depends on the angle α between current and magnetization, via the angular dependence of the resistivity[66]

$$\rho(\alpha) = \rho_\perp + (\rho_\parallel - \rho_\perp)\cos^2\alpha = \rho_\perp + \Delta\rho_{\text{abs}}\cos^2\alpha, \qquad (6)$$

where $\rho_\perp$ and $\rho_\parallel$ denote the resistivities for perpendicular and parallel orientation for magnetization and current, respectively, and $\Delta\rho_{\text{abs}} = (\rho_\parallel - \rho_\perp)$ (for Co, $\Delta\rho_{\text{abs}} > 0$). In fact, all magnetic multilayers show such an angular dependence in the case of magnetic saturation. For a random spontaneous in-plane orientation of the magnetization, we have

$$\rho(H = 0) = \rho(0) = \rho_\perp + 1/2\Delta\rho_{\text{abs}}. \qquad (7)$$

This can be used to detect the spontaneous orientation of the magnetization relative to the layer plane. If, in the case of dominating in-plane anisotropy, the magnetization is randomly oriented in the layer plane in a domains pattern, ρ increases with an increasing magnetic field applied parallel to the layer plane by $1/2\Delta\rho_{\text{abs}}$ up to $\rho_\parallel$, and decreases by $1/2\Delta\rho_{\text{abs}}$ down to $\rho_\perp$ if the magnetic field is directed perpendicular to the layer plane. The saturation fields mirror saturation of the magnetization as they appear in the magnetization curves. If, on the other hand, the magnetization is spontaneously oriented perpendicular to the layer plane, we have

$$\rho(0) = \rho_\perp, \qquad (8)$$

independently from an eventual existence of a multidomain state. Since the domains disappear in a sufficiently high perpendicular field, while the magnetization retains its perpendicular orientation, ρ does not vary with the field. For an in-plane field, ρ increases by $\Delta\rho_{\text{abs}}$ to $\rho_\parallel$ and saturates at $H_S^\parallel$.

Figures 7(a) and 7(b) show the longitudinal and perpendicular magnetoresistance of two representative multilayer samples CeH_2/Co at different temperatures. In addition to the AMR dominating in magnetic fields up to 15 kOe, there is a high-field contribution which is independent of the field orientation and varies linearly with the field in the available range (up to 70 kOe). Here, we focus on the AMR. It behaves very similarly as we expect from our preceding discussion. For the multilayer [15 Å CeH_2/24 Å Co]×50, which according to Sec. IV shows an in-plane magnetic easy axis, the parallel magnetoresistance increases and saturates in a relatively small field (~2 kOe), disregarding the high-field contribution. In a perpendicular field, saturation of the magnetoresistance is reached in a considerably higher field $H_S^\perp$ only. In this case, the initial increase suggests that, starting from an in-plane multidomain configuration, the magnetic field first creates an important component of the magnetization parallel to the current, prior to turning it out of plane into the perpendicular direction. This may be due to a small misaligned component of the external field. The extrapolation of the high-field curves to zero field reveals that the relation for $\rho(0)$ given in Eq. (7) is rather well obeyed. A similar behavior is observed for the multilayer [15 Å CeH_2/14 Å Co]×77 at 100 and 200 K, except that the high-field part of the magnetoresistance now displays a positive slope [Fig. 7(b)]. At 4.2 K however, the magnetoresistance curves are distinctly modified. The slope of the high-field component now is negative. Furthermore, the anisotropic part in the curves now is consistent with the observation (Sec. IV) that, at this temperature, the sample adopts a configuration of magnetic domains magnetized perpendicularly to the layer planes: the relation $\rho(0) = \rho_\perp$ [Eq. (8)] is well obeyed, there is no field dependence for the perpendicular case, disregarding the superimposed high-field part; the longitudinal magnetoresistance saturates at a relatively high magnetic field (~9.5 kOe, compare to Fig. 2).

Figure 7 shows that the relative magnetoresistance $\Delta\rho_{\text{abs}}/\rho$ decreases with increasing temperature. This is a consequence of the resistivity increase due to phonon scattering. In addition, the absolute magnetoresistance $\Delta\rho_{\text{abs}}$ decreases with increasing temperature, which is a common observation for ferromagnetic alloys. This is explained by the temperature-dependent mutual cancellation of non-correlated contributions to anisotropic scattering.[65]

As we have mentioned, the CeH_2/Co multilayers present an additional contribution to the magnetoresistance which adds to the AMR part and can be isolated in sufficiently high magnetic fields (Fig. 7). It does not depend on the relative orientation of field and current and varies approximately linearly with the field; it can increase or decrease, depending on the thickness of the Co sublayers and/or temperature. The effect is under further investigation. Preliminary measurements in magnetic fields up to 350 kOe show deviations

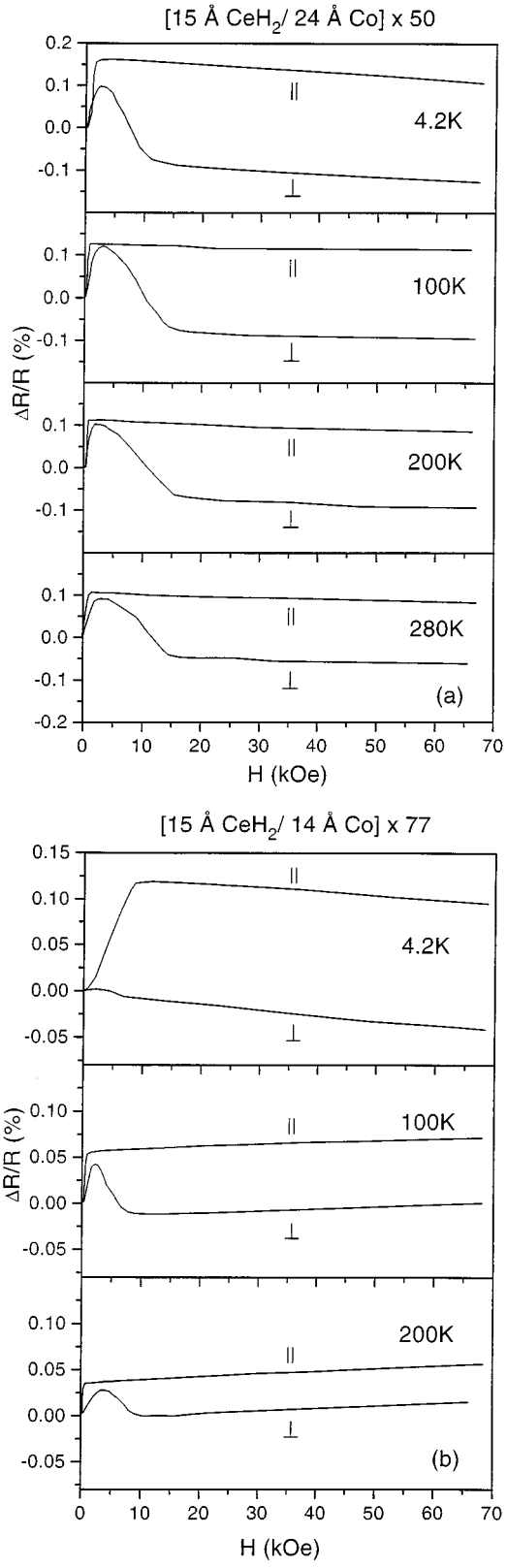

FIG. 7. Longitudinal and perpendicular magnetoresistance of two CeH_2/Co multilayers with Co-layer thicknesses of 24 and 14 Å at different temperatures.

from a linear variation.[67] A similar high-field magnetoresistance has been observed in Ni/Ti, NiC/Ti, and Co/Cu multilayers[68] but remains to be explained.

The present multilayer system combines the component

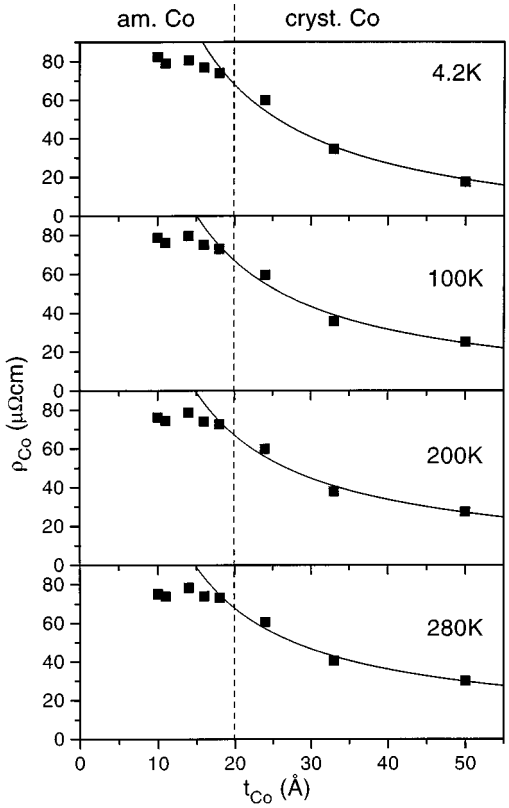

FIG. 8. Electrical resistivity of the Co sublayers, ρ_{Co}, in CeH_2/Co multilayers (CeH_2-layer thickness 15 Å) as a function of t_{Co} at different temperatures. The lines are fits to the form $\rho_{Co} \propto 1/t_{Co}$.

CeH_2 with a high resistivity and the component Co with a relatively low resistivity. This can be used for a separation of the two contributions to the total resistivity. In the simplest case, if interfacial electron scattering can be neglected, the resistivity ρ of a multilayer is that of two resistors in parallel:

$$\frac{\Lambda}{\rho} = \frac{t_{CeH}}{\rho_{CeH}} + \frac{t_{Co}}{\rho_{Co}} \tag{9}$$

with $\Lambda = t_{CeH} + t_{Co}$. Plots of Λ/ρ versus t_{CeH} (9 Å$\leqslant t_{CeH} \leqslant$34 Å) at constant t_{Co}=24 Å for different temperatures (not reproduced here) show that a linear relationship is well obeyed, which indicates that the resistivity of the CeH_2 sublayers is independent of their thickness. The result is $\rho_{CeH} \approx 900\ \mu\Omega$ cm nearly independent of the temperature. It is this high value which is responsible for the relatively small magnetoresistances of the system (Fig. 7); in pure Co layers, for example, magnetoresistances amount to several percent. The high resistivity ρ_{CeH} indicates that the CeH_2 layers are close to the well-known metal-to-semiconductor transition of the material, the behavior still being metallic. In contrast, plots Λ/ρ versus t_{Co} at constant t_{CeH} do not yield straight lines, which shows that the resistivity of the Co sublayers depends on their thickness. Figure 8 shows this dependence as it results from Eq. (9) for t_{CeH}=15 Å at different temperatures. Two regimes are observed: ρ_{Co} is constant near 80 $\mu\Omega$ cm at thicknesses $t_{Co}<20$ Å where Co is amorphous, but varies $\propto 1/t_{Co}$ for larger thicknesses due to a scattering

contribution of the interfaces. For the crystalline Co sublayers the electron mean free path must at least be on the order of their thickness.

B. Extraordinary Hall effect

The Hall resistivity of magnetic materials is composed of the ordinary Hall effect due to the Lorentz force and the extraordinary Hall effect (EHE) based on the spin-orbital coupling:

$$\rho_H = R_0 H + R_S 4\pi M. \tag{10}$$

Here, R_0 and R_S denote the respective Hall coefficients, H is the applied magnetic field and M the magnetization. Our objective is an investigation of the second component, the EHE. (Due to its proportionality to the magnetization, it provides a convenient way to determine the magnetic saturation field of a sample. In fact, the perpendicular fields $H_S^{\perp}$ resulting from the measured extraordinary Hall resistivity of the CeH_2/Co multilayers agree very well with the corresponding data in Fig. 5 deduced from the magnetization curves.) In *homogeneous* magnetic materials, a simple scaling relation between the extraordinary Hall coefficient and the ordinary resistivity ρ holds:[69]

$$R_S = A\rho + B\rho^2. \tag{11}$$

The origin is well understood. Spin-orbit coupling breaks the time symmetry. As a consequence, the scattering matrix contains an asymmetric term with respect to incident and scattered wave vectors, named skew scattering; it gives rise to the first term in Eq. (11). A second effect of spin-orbital coupling is of purely quantum-mechanical nature. Due to the noncommutivity between the position operator and the spin-orbit Hamiltonian, an anomalous velocity term arises which contributes to the EHE in the form of the second term in Eq. (11) known as side jump.

For homogeneous magnetic materials, the validity of the scaling relation in Eq. (11) has been well verified. However, it is a matter of actual discussion[70] whether this relation holds for magnetically inhomogeneous solids such as artificial layered structures consisting of alternately magnetic and nonmagnetic components. According to a recent investigation by Tsui *et al.*,[71] for example, the quadratic scaling relation $R_S \propto \rho^2$ is obeyed in Co/Cu superlattices. This means that Eq. (11) (in the limit that side jump dominates electron scattering) is valid in this system. On the other hand, Zhang,[35] in a calculation based on the Kubo formalism, has recently come to the conclusion that the scaling relation for the side-jump term in Eq. (11) is not valid for magnetic multilayers in general, but only in exceptional cases. One such case is the local limit, where the electron mean free path is small as compared to the thickness of the individual component layers.

The Hall effect of the CeH_2/Co multilayers was measured in conventional geometry, i.e. with the magnetic field H applied in the growth direction and the driving current and Hall voltage in the plane of the layers. The ordinary Hall coefficients R_0 were found to lie in between those of 2000-Å-thick layers of the constituent materials CeH_2 and Co. The extraordinary Hall coefficients R_S were determined from the measured Hall resistivities $R_S 4\pi M_S$ and saturation magnetizations M_S, hence R_S does not depend on H. To test the validity of Eq. (11) for the present case, we display in Fig. 9, for samples with varying Co-layer thickness and constant CeH_2-layer thickness $t_{CeH} = 15$ Å, the extraordinary Hall coefficient divided by the multilayer resistivity, R_S/ρ, as function of the resistivity ρ at different temperatures. The data point to the existence of two regimes, related to multilayers with crystalline or amorphous Co sublayers, respectively, with a borderline defined by ρ between about 120 and 150 $\mu\Omega$ cm. In each regime, the scaling relation in Eq. (11) is obeyed, both skew scattering and side jump contribute to electron scattering; A is on the order of 10^{-6}cm^3/emu and B on the order of 10^{-9}cm$^2/\mu\Omega$ emu.

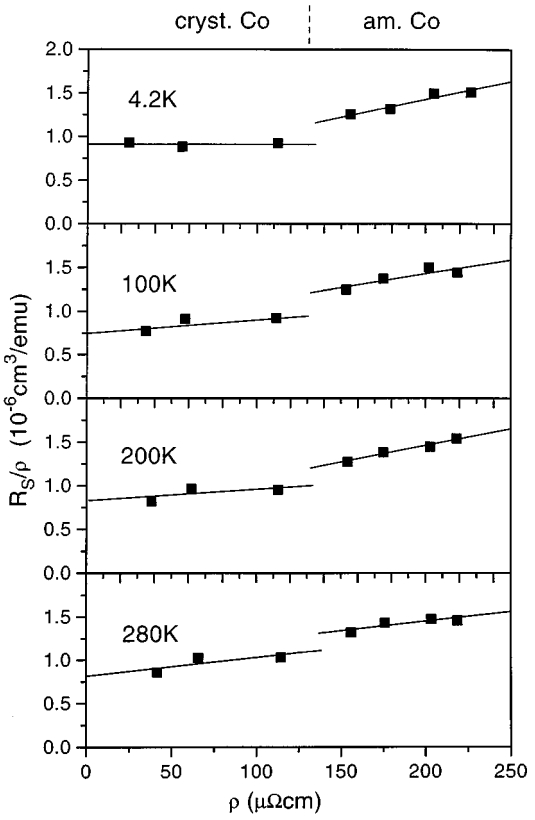

FIG. 9. Extraordinary Hall coefficient R_S of CeH_2/Co multilayers (CeH_2-layer thickness 15 Å) divided by the multilayer resistivity ρ as a function of ρ at different temperatures.

It is not obvious how the validity of the functional dependence of Eq. (11) in the multilayer system under consideration can be substantiated in the framework of Zhang's calculation.[35] The requirement of the local limit may be fulfilled in the regime of the amorphous Co sublayers, but certainly not in the regime where Co is crystalline, i.e., for thicknesses t_{Co} between 20 and 53 Å. In this case a substantial contribution to electron scattering comes from scattering at the interfaces, as we have indicated above, which means that the electron mean free path is not small as compared to the Co-layer thickness t_{Co}. Let us mention (data not shown) that the extraordinary Hall coefficient R_S decreases with t_{Co} qualitatively in a similar way as ρ_{Co} (see Fig. 8), which means that interfacial scattering is an important mechanism for R_S, too, if Co is crystalline. In this case, the sidejump coefficient B increases slightly with temperature which may

reflect the increasing importance of electron-phonon scattering in Co for R_S, as in the case of the resistivity $\rho(T)$. In the regime of amorphous Co, where electron scattering occurs in the volume of both constituents, the sidejump coefficient B is larger than in the case of crystalline Co. Finally, we mention that the R_S-ρ scaling relation [Eq. (11)] is well obeyed in a 2000-Å-thick Co layer. For this layer, R_S varies between 2 and 6×10^{-6} $\mu\Omega\,\mathrm{cm}^4$/emu and ρ between 6 and 12 $\mu\Omega$ cm as a function of temperature between 4.2 and 300 K. The coefficients obtained from a fit to Eq. (11) are $A=2.8\times10^{-7}$ cm^3/emu and $B=1.5\times10^{-7}$ $\mathrm{cm}^2/\mu\Omega$ emu. Note that in particular B is 2 orders of magnitude larger than in the CeH_2/Co multilayers. This means that electron scatting from side jump is considerably more effective in the thick Co layer than in the multilayers.

VI. CONCLUSIONS

Multilayers of periodically stacked CeH_x ($x\approx2$) and Co films can be prepared with sharp interfaces by reactive ion-beam sputtering in a hydrogen atmosphere. Arguments based on solution enthalpies and comparison with other hydrided multilayers suggest that essentially only the Ce layers take up the hydrogen. The individual CeH_2 and Co layers grow in a (111)-textured fcc-structure above critical thicknesses of 15 and 20 Å, respectively, and in an amorphous structure below these thicknesses. The temperature dependence of the magnetization follows a spin-wave law for a three-dimensional ferromagnetic solid, with a considerably enhanced spin-wave parameter compared to bulk fcc Co. The saturation magnetization and the spin-wave parameter vary continuously through the crystalline-to-amorphous transition of the Co sublayers. This is in contrast to the behavior of multilayer systems based on Fe, where the transition to the amorphous Fe phase is accompanied by a drastic reduction of the saturation magnetization. This behavior demonstrates that the electronic configurations of amorphous Co and Fe are closely related to those of the fcc phases of the bulk metals. A magnetically dead zone is identified in the Co layers at the interfaces with CeH_2. It may result from hybridization effects of the electronic d states in the intermixed region.

At low temperatures, below a critical thickness of about 17 Å, the magnetization is spontaneously oriented perpendicular to the layer planes in a multidomain configuration. The magnetization turns into the layer planes between 50 and 100 K. It is demonstrated that phenomenologically the orientation of the magnetic easy axis is determined by the competition of a strong interface contribution to the magnetic anisotropy energy, which supports a perpendicular easy axis, and the shape anisotropy together with an additional volume anisotropy, which advocate an in-plane easy axis. The mechanisms behind the counteracting surface and extra volume anisotropies could not be identified. Comparison with the recently studied CeH_2/Fe multilayers[25] reveal interesting differences. For example, the perpendicular magnetic ground state is stable up to considerably larger Fe-layer thicknesses, due to a magnetostatic interaction of the perpendicular domains across the CeH_2 spacer. Furthermore, in this system the temperature-driven reorientation of the magnetization occurs at a well-defined temperature which depends on the thickness of *both* sublayers.

The magnetic anisotropy of the multilayers and resulting the spontaneous orientation of the magnetization with respect to the layer planes derived from the study of the magnetization curves is reflected in the appearance of an anisotropic magnetoresistance. The extraordinary Hall effect is composed of contributions from skew scattering and side jump. The extraordinary Hall coefficient scales with the ordinary electrical resistivity. The data point to the existence of two regimes, related to crystalline or amorphous Co sublayers.

ACKNOWLEDGMENTS

This work was supported by the Deutsche Forschungsgemeinschaft within SFB 345. We thank W. Lohstroh for useful discussions and J. C. Ousset for interesting correspondence.

*Present address: Hahn-Meitner-Institut Berlin, Glienicker Str. 100, 14109 Berlin, Germany.

[1] *Ultrathin Magnetic Structures I*, edited by J. A. C. Bland and B. Heinrich (Springer, Berlin, 1994).
[2] P. Bruno, Phys. Rev. B **39**, 865 (1989).
[3] G. H. O. Daalderop, P. J. Kelly, and M. F. H. Schuurmans, Phys. Rev. B. **42**, 7270 (1990); **44**, 12 054 (1991).
[4] D. Weller, Y. Wu, J. Stöhr, M. G. Samant, B. D. Hersmeier, and C. Chappert, Phys. Rev. B **49**, 12 888 (1994).
[5] D. Weller, J. Stöhr, R. Nakajima, A. Carl, M. G. Samant, C. Chappert, R. Mégy, P. Beauvillain, P. Veillet, and G. A. Held, Phys. Rev. Lett. **75**, 3752 (1995).
[6] G. H. O. Daalderop, P. J. Kelly, and M. F. H. Schuurmans, *Ultrathin Magnetic Structures* (Ref. 1), p. 40.
[7] W. J. M. de Jonge, P. J. H. Bloemen, and F. J. A. den Broeder, *Ultrathin Magnetic Structures* (Ref. 1), p. 65.
[8] L. Néel, J. Phys. Rad. **15**, 225 (1954).
[9] D. P. Pappas, K.-P. Kämper, and H. Hopster, Phys. Rev. Lett. **64**, 3179 (1990).
[10] R. Allenspach and A. Bischof, Phys. Rev. Lett. **69**, 3385 (1992).
[11] Z. Q. Qiu, J. Pearson, and S. D. Bader, Phys. Rev. Lett. **70**, 1006 (1993); S. D. Bader, Donqui Li, and Z. Q. Qiu, J. Appl. Phys. **76**, 6419 (1994).
[12] See, e.g., A. Moschel and K. D. Usadel, Phys. Rev. B **49**, 12 868 (1994), and references therein.
[13] P. J. Jensen and K. H. Bennemann, Phys. Rev. B **42**, 849 (1990); Solid State Commun. **83**, 1057 (1992).
[14] I. Booth, A. B. MacIsaac, and J. P. Whitehead, Phys. Rev. Lett. **75**, 950 (1995).
[15] N. D. Mermin and H. Wagner, Phys. Rev. Lett. **17**, 1133 (1966).
[16] D. P. Pappas, C. R. Brundle, and H. Hopster, Phys. Rev. B **45**, 8169 (1992).
[17] R. Allenspach, J. Magn. Magn. Mater. **129**, 160 (1994).
[18] Y. Yafet and E. M. Gyorgy, Phys. Rev. B **38**, 9145 (1988).
[19] A. Kashuba and V. L. Pokrovsky, Phys. Rev. Lett. **70**, 3154 (1993); Phys. Rev. B **48**, 10 335 (1993); Ar. Arbanov, V. Kalatsky, V. L. Pokrovsky, and W. M. Saslow, *ibid.* **51**, 1023 (1995).
[20] B. Kaplan and G. A. Gehring, J. Magn. Magn. Mater. **128**, 111 (1993).

[21] H. J. G. Draaisma and W. J. M. de Jonge, J. Appl. Phys. **62**, 3318 (1993).
[22] J. R. Barnes, S. J. O'Shea, M. E. Welland, J.-Y. Kim, J. E. Evetts, and R. E. Somekh, J. Appl. Phys. **76**, 2974 (1994).
[23] A. Berger and H. Hopster, Phys. Rev. Lett. **76**, 519 (1996).
[24] For the properties of cerium hydride, see, for example, R. R. Arons, in *Landolt-Börnstein, Zahlenwerte und Funktionen aus Naturwissenschaften und Technik*, edited by K. H. Hellwege and A. M. Hellwege (Springer, Berlin, 1991), Vol. III/19d1, p. 330.
[25] O. Schulte, F. Klose, and W. Felsch, Phys. Rev. B **52**, 6480 (1995).
[26] Ph. Bauer, F. Klose, O. Schulte, and W. Felsch, J. Magn. Magn. Mater. **138**, 163 (1994).
[27] K. Cherifi, C. Dufour, M. Piecuch, A. Bruson, Ph. Bauer, G. Marchal, and Ph. Mangin, J. Magn. Magn. Mater. **93**, 609 (1991).
[28] Y. J. Wang and W. Kleeman, Phys. Rev. B **44**, 5132 (1991).
[29] L. T. Baczewski, M. Piecuch, J. Durand, G. Marchal, and P. Delcroix, Phys. Rev. B **40**, 11 237 (1989).
[30] K. Mibu, N. Hosoito, and T. Shinjo, Hyperfine Interact. **54**, 831 (1990).
[31] W. Lohstroh *et al.*, Diplomarteit, Universität Göttingen, 1996.
[32] F. Klose, O. Schulte, F. Rose, W. Felsch, S. Pizzini, C. Giorgetti, F. Baudelet, E. Dartyge, G. Krill, and A. Fontaine, Phys. Rev. B **50**, 6174 (1994).
[33] O. Schulte *et al.* (unpublished).
[34] F. Klose, J. Thiele, A. Schurian, O. Schulte, M. Steins, O. Bremert, and W. Felsch, Z. Phys. B **90**, 79 (1993).
[35] S. Zhang, Phys. Rev. B **51**, 3632 (1995).
[36] M. A. Vannice, J. Catal. **37**, 449 (1975); G. A. Somorjai, Catal. Rev. Sci. Eng. **23**, 189 (1981).
[37] R. Griessen and T. Riesterer, in *Hydrogen in Intermetallic Compounds*, edited by L. Schlapbach (Springer, Berlin, 1988), Vol. I, p. 266.
[38] J. Landes, Ch. Sauer, B. Kabius, and W. Zinn, Phys. Rev. B **44**, 8342 (1991).
[39] M. Grimsditch, E. E. Fullerton, and I. Schuller, Mater. Res. Soc. Symp. Proc. **308**, 685 (1993).
[40] The deviations may be traced back to elastic constraints at the boundary with the substrate [J. Steiger *et al.*, Phys. Rev. B **49**, 5570 (1994); P. F. Miceli *et al.*, J. Mater. Res. **6**, 964 (1991)] or due to electron transfer at the interface with a different material [B. Hjörvarsson *et al.*, Phys. Rev. B **43**, 6440 (1991)].
[41] H. Zabel and A. Weidinger, Comments Condens. Matter Phys. **17**, 239 (1995); A. Weidinger, D. Nagengast, Ch. Rehm, F. Klose, and B. Pietzak, Thin Solid Films **275**, 48 (1996).
[42] Y. Fukai, *The Metal-Hydrogen System* (Springer, Berlin, 1993), p. 96.
[43] D. Nagengast, J. Erxmeyer, F. Klose, Ch. Rehm, P. Kuschnerus, G. Dortmann, and A. Weidinger, J. Alloys Compd. **231**, 307 (1995).
[44] *Binary Alloy Phase Diagrams*, edited by T. B. Massalski, J. L. Murray, L. H. Bennett, H. Baker, and L. Kacprzak, (American Society for Metals, Metals Park, OH, 1995), pp. 1708 and 1192.
[45] L. G. Parratt, Phys. Rev. **95**, 359 (1954); L. Nevot and P. Croce, Rev. Phys. Appl. **15**, 761 (1980).
[46] *Landolt-Börnstein, Zahlenwerte und Funktionen aus Naturwissenschaften und Technik* (Springer, Berlin, 1986), Vol. III/19a, p. 75.
[47] S. Handschuh, J. Landes, U. Köbler, Ch. Sauer, G. Kisters, A. Fuss, and W. Zinn, J. Magn. Magn. Mater. **119**, 254 (1993).
[48] J. Thiele, F. Klose, A. Schurian, O. Schulte, W. Felsch, and O. Bremert, J. Magn. Magn. Mater. **119**, 141 (1993).
[49] F. Rose, O. Schulte, P. Schaaf, W. Lohstroh, and W. Felsch, Appl. Phys. A **63**, 183 (1996).
[50] For an early investigation, see W. Felsch, Z. Phys. **219**, 280 (1969); Z. Angew. Phys. **30**, 275 (1970).
[51] R. Lorenz and J. Hafner, J. Magn. Magn. Mater. **139**, 209 (1995).
[52] R. F. Sabiryanov, S. K. Bose, and O. N. Mryasov, Phys. Rev. B **51**, 8958 (1995).
[53] Y. Kakehashi, Phys. Rev. B **41**, 9207 (1990); M. Yu, Y. Kakehashi, and H. Tanaka, *ibid.* **49**, 352 (1994).
[54] H. Tanaka, S. Takayama, M. Hasegawa, T. Fukunaga, U. Mizutanai, A. Fujita, and K. Fukamichi, Phys. Rev. B **47**, 2671 (1993).
[55] Y. Kakehashi and M. Yu, Phys. Rev. B **49**, 15 076 (1994).
[56] U. Mizutani, M. Hasegawa, K. Fukamichi, Y. Hattory, Y. Yamada, H. Tanaka, and S. Takayama, Phys. Rev. B **47**, 2678 (1993); K. Fukamichi, T. Goto, and U. Mizutani, IEEE Trans. Magn. **MAG-23**, 3590 (1987).
[57] A. Suna, J. Appl. Phys. **59**, 313 (1986).
[58] M. T. Johnson, R. Jungblut, P. J. Kelly, and F. J. A. den Broeder, J. Magn. Magn. Mater. **148**, 118 (1995).
[59] C. Chappert and P. Bruno, J. Appl. Phys. **64**, 5736 (1988).
[60] O. Schulte, A. Traverse, and J. Mimault (unpublished).
[61] E. Boroch and E. Kaldis, Z. Phys. Chemie, Neue Folge **163**, 117 (1989).
[62] S. Chikazumi and S. H. Charap, *Physics of Magnetism* (Krieger, Malabar, 1986).
[63] H. Takahashi, S. Tsunashima, S. Iwata, and S. Uchiyama, Jpn. J. Appl. Phys. **32**, L1328 (1993).
[64] G. Bochi, O. Song, and R. C. O'Handley, Phys. Rev. B **50**, 2043 (1994).
[65] P. Ciureanu, in *Thin Film Resistive Sensors*, edited by P. Ciureanu and S. Middelhoek (IOP, Bristol, 1992), p. 253.
[66] I. A. Campbell and A. Fert, in *Ferromagnetic Materials*, edited by E. P. Wohlfarth (North-Holland, Amsterdam, 1982).
[67] J. C. Ousset *et al.* (unpublished).
[68] A. Sdaq, J. M. Broto, H. Rakoto, J. C. Ousset, B. Raquet, B. Vidal, Z. Jiang, J. F. Bobo, M. Piecuch, and B. Baylac, J. Magn. Magn. Mater. **121**, 409 (1993).
[69] L. Berger and G. Bergmann, in *The Hall Effect and Its Applications*, edited by C. L. Chien and C. R. Westgate (Plenum Press, New York, 1980), p. 180.
[70] See, e.g., H. Sato, H. Henmi, Y. Kobayashi, Y. Aoki, H. Yamamoto, T. Shinjo, and V. Sechovsky, J. Appl. Phys. **76**, 6919 (1994); H. Sato, Y. Kobayashi, Y. Aoki, Y. Saito, and K. Inomata, Phys. Rev. B **52**, R9823 (1995).
[71] F. Tsui, B. Chen, D. Barlett, R. Clarke, and C. Uher, Phys. Rev. Lett. **72**, 740 (1994).